

## Lifetime-Limited Interrogation of Two Independent $^{27}\text{Al}^+$ Clocks Using Correlation Spectroscopy

Ethan R. Clements<sup>1,2,\*</sup>, May E. Kim,<sup>1</sup> Kaifeng Cui<sup>1,3</sup>, Aaron M. Hankin,<sup>1,2,†</sup> Samuel M. Brewer,<sup>1,‡</sup> Jose Valencia,<sup>1,2</sup> Jwo-Sy Chen,<sup>1,2,§</sup> Chin-Wen Chou,<sup>1</sup> David R. Leibrandt<sup>1,2</sup> and David B. Hume<sup>1,||</sup>

<sup>1</sup>National Institute of Standards and Technology, Boulder, Colorado 80305, USA

<sup>2</sup>Department of Physics, University of Colorado, Boulder, Colorado 80305, USA

<sup>3</sup>HEP Division, Argonne National Laboratory, Lemont, Illinois 60439, USA

 (Received 9 July 2020; revised 13 October 2020; accepted 30 October 2020; published 9 December 2020)

Laser decoherence limits the stability of optical clocks by broadening the observable resonance linewidths and adding noise during the dead time between clock probes. Correlation spectroscopy avoids these limitations by measuring correlated atomic transitions between two ensembles, which provides a frequency difference measurement independent of laser noise. Here, we apply this technique to perform stability measurements between two independent clocks based on the  $^1S_0 \leftrightarrow ^3P_0$  transition in  $^{27}\text{Al}^+$ . By stabilizing the dominant sources of differential phase noise between the two clocks, we observe coherence between them during synchronous Ramsey interrogations as long as 8 s at a frequency of  $1.12 \times 10^{15}$  Hz. The observed contrast in the correlation spectroscopy signal is consistent with the 20.6 s  $^3P_0$  state lifetime and represents a measurement instability of  $(1.8 \pm 0.5) \times 10^{-16} / \sqrt{\tau/s}$  for averaging periods longer than the probe duration when dead time is negligible.

DOI: [10.1103/PhysRevLett.125.243602](https://doi.org/10.1103/PhysRevLett.125.243602)

High-stability frequency comparisons are the basis of many applications of optical atomic clocks including time and frequency metrology [1], relativistic geodesy [2], and tests of fundamental physics [3]. Measurements with optical clocks are typically performed by stabilizing a laser frequency to an atomic resonance based on measured atomic transition probabilities [4]. Here, laser frequency noise contributes intrinsically to measurement instability, because it limits the probe duration [5,6], effectively broadening the linewidth of the atomic resonance [7]. It also introduces noise during the dead time between clock interrogations [8]. Recent work has improved laser stability [9] and used synchronized interrogation techniques to remove Dick effect noise [10–12] but has not yet reached the stability required to probe many atomic clock transitions at the atomic species' natural linewidths. Correlation spectroscopy is an alternative frequency comparison technique that avoids these limitations by simultaneous interrogation of two atoms (or two atomic ensembles) with the same laser, which allows for common-mode cancellation of laser noise and probe times longer than the laser coherence time.

To illustrate the laser-noise limitation, consider frequency measurements on a two-level system with states  $|\downarrow\rangle$  and  $|\uparrow\rangle$  [7]. A typical Ramsey sequence beginning from  $|\downarrow\rangle$  involves two  $\pi/2$  pulses with a controlled laser phase difference  $\phi$  separated by the probe duration  $T_R$  [13]. We assume each  $\pi/2$  pulse has a duration negligible compared to  $T_R$ . A measurement of  $\hat{\sigma}_z = |\uparrow\rangle\langle\uparrow| - |\downarrow\rangle\langle\downarrow|$  at the end of this sequence has expectation value

$\langle\hat{\sigma}_z\rangle = \cos[(\omega_L - \omega_0)T_R + \phi]$ , where  $\omega_L$  is the laser frequency and  $\omega_0$  is the atomic resonance frequency. Atom-laser decoherence (for example, due to laser frequency fluctuations or atomic spontaneous emission) alters this picture by reducing the contrast of the Ramsey fringe by a factor  $C(T_R) < 1$ , which depends on the probe duration. In many optical clocks, including the  $^{27}\text{Al}^+$  clocks in this Letter, decoherence over the relevant timescales is dominated by flicker-frequency noise of the laser [4]. This limits the optimum probe duration, which has been evaluated analytically and through numerical simulation [5,6,14,15]. The reduced contrast  $C(T_R)$  due to flicker-frequency noise can be estimated based on the assumption of Gaussian-distributed phase fluctuations as  $C(T_R) = e^{-(\sigma_0\omega_0 T_R)^2/2}$ , where  $\sigma_0$  is the fractional flicker noise floor of the Allan deviation. The instability at long averaging times  $\tau$  is then given by

$$\sigma(\tau) = \frac{1}{\omega_0\sqrt{T_R\tau}} e^{(\sigma_0\omega_0 T_R)^2/2}, \quad (1)$$

which has a minimum at  $T_R = 1/\sqrt{2}\sigma_0\omega_0$ .

To avoid this limit, in correlation spectroscopy, two atoms or atomic ensembles are probed simultaneously with the same laser, and their frequency difference is determined by measurements of the parity operator,  $\hat{\Pi} = \hat{\sigma}_{z,1} \otimes \hat{\sigma}_{z,2}$ . For unentangled atoms in a pure quantum state,  $\langle\hat{\Pi}\rangle = \langle\hat{\sigma}_{z,1}\rangle\langle\hat{\sigma}_{z,2}\rangle = \cos(\Delta_1 T_R + \phi_1) \cos(\Delta_2 T_R + \phi_2)$ , where we have defined  $\Delta_i \equiv \omega_L - \omega_{0,i}$  and  $i$  is an index that refers to each atom. We can separate  $\langle\hat{\Pi}\rangle$  into terms that

depend on the sum and difference frequency detunings  $\Delta_{\pm} \equiv \Delta_1 \pm \Delta_2$  and phases  $\phi_{\pm} \equiv \phi_1 \pm \phi_2$  such that

$$\langle \hat{\Pi} \rangle = \frac{1}{2} [\cos(\Delta_+ T_R + \phi_+) + \cos(\Delta_- T_R + \phi_-)]. \quad (2)$$

At probe durations long compared to the laser coherence time, the first term in Eq. (2) averages to zero. The fundamental limit in coherence time for a particular clock transition is given by the spontaneous decay rate  $\Gamma$  (typically, the rate of decay from the excited state). If a spontaneous decay event occurs during the Ramsey probe duration, the second Ramsey  $\pi/2$  pulse places the atom in an equal superposition of up and down. Including spontaneous decay and assuming no laser coherence, Eq. (2) becomes

$$\langle \hat{\Pi} \rangle = \frac{1}{2} e^{-\Gamma T_R} \cos(\Delta_- T_R + \phi_-). \quad (3)$$

Since  $\Delta_- = \omega_{0,1} - \omega_{0,2}$ , Eq. (3) represents a direct atom-atom frequency measurement that is independent of the laser noise. The fractional instability of a frequency ratio measurement at this lifetime limit is given by

$$\sigma_C(\tau) = \frac{2}{\omega_0 \sqrt{T_R \tau}} e^{\Gamma T_R}, \quad (4)$$

where we have used  $\omega_{0,i} \approx \omega_0$ . The optimum probe duration for a correlation spectroscopy comparison is then  $T_{R,\text{opt}} = 1/(2\Gamma)$  [15].

Previous implementations of correlation spectroscopy for optical clocks used two or more ions [16–21] or neutral atomic ensembles [22,23] confined in the same trap. In these experiments, the atoms were colocated to within a few microns such that differential effects including optical path length fluctuations and noise due to variations in the ambient electromagnetic field were naturally suppressed. Using this technique for many clock applications requires implementation in spatially separated optical clocks, where differential noise can limit their relative coherence. Here, by suppressing sources of differential noise, in both the probe laser beams and the atomic resonance frequencies, we demonstrate correlation spectroscopy between two independent clocks and observe linewidths approaching the ultimate limit of resolution from the  $^{27}\text{Al}^+ \ ^3P_0$  excited-state lifetime of 20.6 s [24].

We implement correlation spectroscopy using two optical atomic clocks based on quantum logic spectroscopy of the  $^1S_0 \leftrightarrow ^3P_0$  transition in  $^{27}\text{Al}^+$ . A key difference between the two optical clocks is the choice of qubit species, which is used for sympathetic cooling and state readout [25]. One of these systems, using  $^{25}\text{Mg}^+$  as the qubit, has recently been evaluated to have a systematic fractional frequency uncertainty of  $\Delta f/f = 9.4 \times 10^{-19}$  [26]. The second, using  $^{40}\text{Ca}^+$  as a qubit, is a newly developed clock with improved

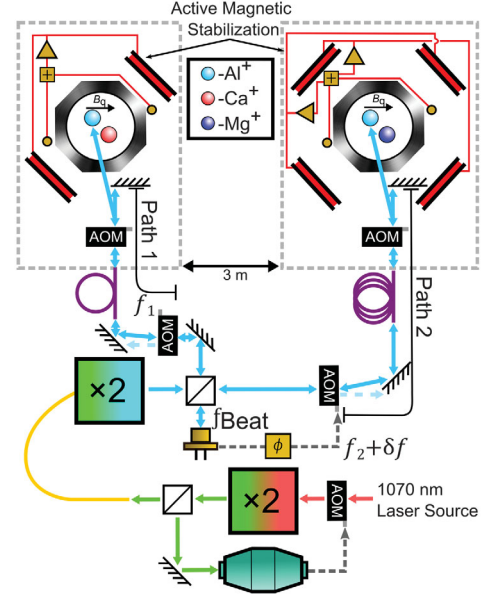


FIG. 1. Schematic of the correlation spectroscopy experiment, including the laser path-length stabilization and active magnetic field stabilization setups. Here  $f_{\text{Beat}} = 2(f_1 - f_2)$  is phase locked to a maser-referenced 10 MHz signal, and the relative phase is corrected by modulating the path 2 AOM, denoted by  $f_2 + \delta f$ . The magnetic field is stabilized using measurements from single-axis flux gate sensors (shown as yellow circles) oriented along the quantization axis  $B_q$ . In the  $^{25}\text{Mg}^+ / ^{27}\text{Al}^+$  clock, two pairs of coils are used, while in the  $^{40}\text{Ca}^+ / ^{27}\text{Al}^+$  system there is only one. Boxes labeled  $\times 2$  denote frequency doubling of the input light where the final light sent to the atomic clocks is at 267.4 nm.

control of some systematic uncertainties, but its error budget has not been fully evaluated. In what follows, we identify these two systems as  $^{25}\text{Mg}^+ / ^{27}\text{Al}^+$  and  $^{40}\text{Ca}^+ / ^{27}\text{Al}^+$ , respectively.

The two clocks are located on optical tables spaced roughly 3 m apart. A diagram of the experiment is given in Fig. 1(a). All laser systems used for cooling and manipulation of the qubit ions are independent; however, the  $^{27}\text{Al}^+$  laser systems ( $^3P_1$  and  $^3P_0$ ) both share a common source for the two clocks. The 267 nm laser light used to drive the  $^1S_0 \leftrightarrow ^3P_0$  clock transition is generated on the  $^{40}\text{Ca}^+ / ^{27}\text{Al}^+$  optical table and sent to the  $^{25}\text{Mg}^+ / ^{27}\text{Al}^+$  table via a 6-m-long UV-cured photonic crystal fiber [27].

Using the same laser source for the two clocks allows for precise control of the differential phase in the probe pulses by active suppression of Doppler noise in the optical fibers and free-space optical paths [28,29]. A diagram of the path-length stabilization setup is given in Fig. 1, where the total path length between the two ions is  $\approx 10$  m. Part of the laser beams are retroreflected close to where they enter the two vacuum systems and form a beat note near the output of the UV frequency doubler. The relative phase noise in this beat note is measured using an avalanche photodiode and is stabilized by

controlling an acousto-optic modulator (AOM) frequency in the  $^{25}\text{Mg}^+/\text{}^{27}\text{Al}^+$  path. In out-of-loop measurements using a test setup comparable to the setup in Fig. 1, we observe differential phase fluctuations below  $\pi/20$  at Ramsey probe durations as long as 12 s [15]. This residual noise is likely limited by the short, out-of-loop, open-air paths such as those before the ion traps.

Another effect that can limit the atom-atom coherence of the two systems is fluctuations of the local magnetic fields. To minimize the corresponding Zeeman shifts in each clock, we servo the magnetic field based on measurements with multiple flux gate magnetometers placed close to the vacuum chamber and oriented along the clock quantization axis. A linear combination of these measurements is used to estimate the magnetic field at the ion, and corrections are made using a set of Helmholtz coils mounted around each optical table. Using these active stabilization techniques, we reduce the magnetic field noise amplitude to below  $20 \mu\text{G}$  ( $1 \text{ G} = 10^{-4} \text{ T}$ ) for averaging times as long as  $10^3 \text{ s}$  [15].

Both the  $^1S_0$  and  $^3P_0$  states in  $^{27}\text{Al}^+$  have magnetic quantum number  $F = 5/2$ . We performed initial correlation spectroscopy experiments on the  $|^1S_0, m_F = 5/2\rangle \leftrightarrow |^3P_0, m_F = 5/2\rangle$  transition, which has a sensitivity to magnetic fields of  $-4.2 \text{ kHz/G}$ . Through numerical simulations using measured magnetic field noise, we found that this residual magnetic field noise was still a limitation [15]. To further reduce the effect of magnetic field noise, we switched to probing the  $|^1S_0, m_F = 3/2\rangle \leftrightarrow |^3P_0, m_F = 1/2\rangle$  transition. This transition has a sensitivity to magnetic fields of  $0.28 \text{ kHz/G}$ , a factor of 15 reduction in sensitivity compared to the typical clock transition.

During a measurement run, we use the measurement outcome of the previous experimental cycle as projective state preparation for the next such that  $|\downarrow\rangle$  can be either the  $^1S_0$  or  $^3P_0$  state. Parity measurements are made by observing if a transition in each ion state has occurred since the previous interrogation. A parity of  $+1$  corresponds to both atoms making a transition or both not making a transition, whereas a parity of  $-1$  corresponds to only one of the two ions making a transition. To generate the parity fringes seen in Fig. 2, the  $^{40}\text{Ca}^+/\text{}^{27}\text{Al}^+$  clock is interrogated with a constant Ramsey phase  $\phi_1$ , while the  $^{25}\text{Mg}^+/\text{}^{27}\text{Al}^+$  clock scans its phase  $\phi_2$ , relative to the  $^{40}\text{Ca}^+/\text{}^{27}\text{Al}^+$  clock. Scanning the relative phase between the two systems' second  $\pi/2$  pulses allows the coherence between the two systems to be observed. Each point on the fringe is probed  $\gtrsim 50$  times to average down the quantum projection noise.

In these parity phase scans, we observe atom-atom coherence well beyond the coherence time of the laser ( $460 \pm 30 \text{ ms}$ ), which has been measured using a single ion [15]. Because of periodic interruptions from ion loss and other effects [15], the fringes in Fig. 2 accumulate data from multiple runs of the experiment and span total measurement

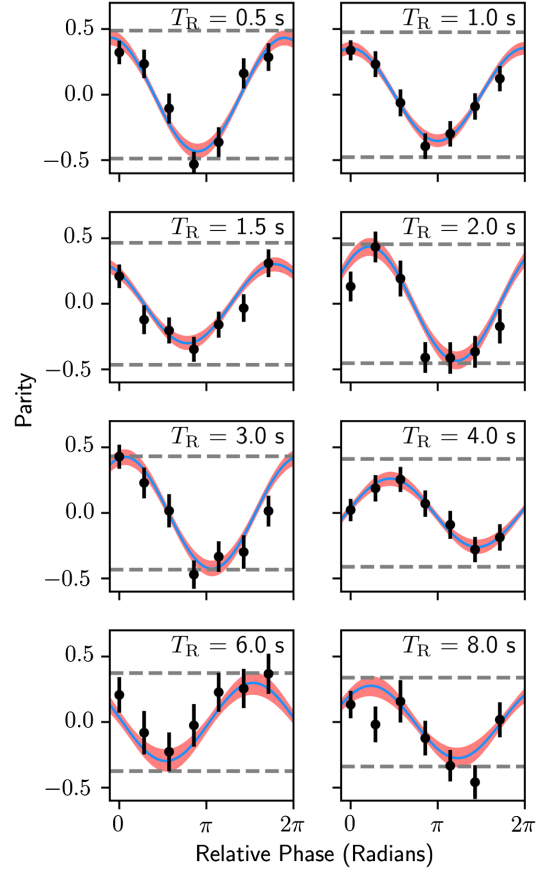


FIG. 2. Parity fringes obtained for Ramsey probe durations between 0.5 and 8 s (upper right labels). Here, the transition used for correlation spectroscopy is the  $|^1S_0, m_F = 3/2\rangle \leftrightarrow |^3P_0, m_F = 1/2\rangle$  transition. Experimental data (dots) are shown with error bars dominated by quantum projection noise. Fits to these parity fringes (lines) and their  $1\sigma$  confidence intervals (shaded region) are determined by resampling the data using nonparametric bootstrapping methods. The maximum obtainable parity amplitude (gray dashed lines) due to the finite lifetime of the two  $^{27}\text{Al}^+$  ions is calculated using Eq. (3).

durations as long as 4 h. The fringe contrast, thus, represents all atom-atom decoherence mechanisms that act on timescales of seconds as well as long-term frequency drifts that act on timescales of hours. To maintain the laser frequency near resonance for the Ramsey  $\pi/2$  pulses between these runs, common-mode adjustments to the laser frequency were made.

Fits of the function  $\langle \hat{\Pi}(\phi_-) \rangle = C \cos(\phi_- - \phi_0)$  to the parity data in Fig. 2 are used to extract the contrast  $C$ , phase  $\phi_0$ , and their associated uncertainties. The uncertainties are obtained by a nonparametric bootstrapping method [15,30]. A plot of the measured contrast as a function of the Ramsey probe duration can be seen in Fig. 3, showing data taken on the less magnetically sensitive  $|^1S_0, m_F = 3/2\rangle \leftrightarrow |^3P_0, m_F = 1/2\rangle$  transition as well as initial data taken on the  $|^1S_0, m_F = 5/2\rangle \leftrightarrow |^3P_0, m_F = 5/2\rangle$

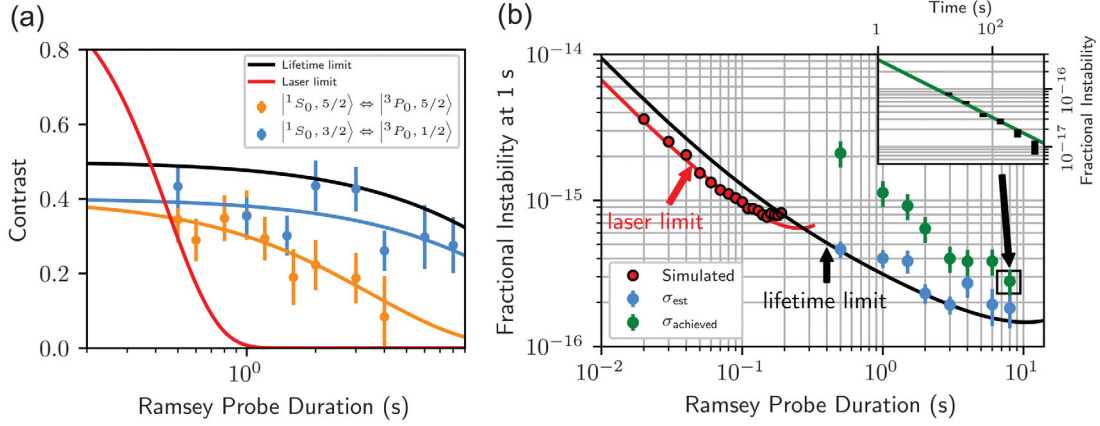


FIG. 3. (a) Contrast as a function of the probe duration. The measured contrast (solid points) and associated uncertainty come from fits to the parity fringes. For comparison, a fit to the laser-coherence-limited Ramsey spectroscopy contrast [15] (red line) and the calculated upper bound on the correlation spectroscopy contrast set by the lifetime limit (black line) are plotted. A fit to the experimental points using the model function  $A \exp^{-T_R/t_d}$  is determined, where  $A$  is the contrast and  $t_d$  is the decay time. Fitting with this function gives  $A = 0.4 \pm 0.04$  and  $t_d = 19 \pm 11$  s for  $|^1S_0, m_F = 3/2\rangle \leftrightarrow |^3P_0, m_F = 1/2\rangle$  and  $A = 0.4 \pm 0.06$  and  $t_d = 4 \pm 2$  s for  $|^1S_0, m_F = 5/2\rangle \leftrightarrow |^3P_0, m_F = 5/2\rangle$ . (b) Comparison of the instability calculations and measurements as a function of probe duration. The instability  $\sigma_{\text{upper}}$  calculated using Eq. (6), is shown with green dots. This can be compared with the instability  $\sigma_{\text{est}}$  determined with Eq. (5) shown with blue dots. A lower bound on the instability is given by the lifetime limit [black line, Eq. (4)], which assumes a randomized laser phase at all probe durations. Also included is an estimate of the instability at the laser-noise limit both from the analytical estimate [red line, Eq. (1)] and a numerical simulation (red points) assuming a flicker-frequency noise floor at  $4.4 \times 10^{-16} \sqrt{\tau/s}$ . Numerical simulations stop at a probe duration of  $\approx 200$  ms due to fringe hops occurring in our numerical simulation. For all theoretical estimates, we assume a dead time of only 0.1 s (the average single-cycle dead time of our clocks), which has negligible impact at longer probe durations. The inset displays the Allan deviation of the frequency ratio measurement at a Ramsey probe duration of 8 s (details and data for other probe durations are given in Supplemental Material [15]).

transition. The noise suppression due to the magnetic field servo is comparable in both of these datasets, and the improvement in the contrast is due to the reduced magnetic sensitivity of the  $|^1S_0, m_F = 3/2\rangle \leftrightarrow |^3P_0, m_F = 1/2\rangle$  transition.

The decay time of the contrast for experiments on the  $|^1S_0, m_F = 3/2\rangle \leftrightarrow |^3P_0, m_F = 1/2\rangle$  transition is measured to be  $t_d = 19 \pm 11$  s. This value is much longer than the measured laser coherence time of  $460 \pm 30$  ms and is consistent with the decay time of 20.6 s expected due to the finite excited-state lifetime. However, we observe a 20(8)% reduction in the contrast from the ideal value of 0.5 set by Eq. (3). We attribute this primarily to errors in the  $^{27}\text{Al}^+$  state preparation and  $\pi$ -pulse infidelity when driving the clock transition.

The contrast of the fringes can be used to estimate the achievable measurement instability for correlation spectroscopy comparisons between the two clocks [18], using

$$\sigma_{\text{est}} = \frac{1}{\omega_0 C(T_R) \sqrt{T_R}}. \quad (5)$$

We find instability as low as  $\sigma_{\text{est}} = (1.8 \pm 0.5) \times 10^{-16} / \sqrt{\tau/s}$  at  $T_R = 8$  s, which corresponds to the achievable instability given the observed contrast if there

is no dead time in the measurement, and all probes were made at the relative phases where the parity slope is the highest. In our experiment, for the longer probe durations, we have negligible overhead due to state preparation and measurement but suffer from frequent interruptions due to collisions with background gas. Furthermore, in these demonstration experiments, some of the duty cycle is spent probing at relative phases with low slope that provide minimal information about the frequency difference of the clocks. An estimate of the achieved measurement instability assumes a total averaging time  $\tau_{\text{tot}}$  including all dead time during the measurement runs and the phase uncertainty  $\sigma_\phi$  determined from the fit of the parity fringe,

$$\sigma_{\text{achieved}} = \frac{\sigma_\phi \sqrt{\tau_{\text{tot}}}}{T_R \omega_0}. \quad (6)$$

For  $T_R = 8$  s, this gives  $(2.8 \pm 0.6) \times 10^{-16} / \sqrt{\tau/s}$  as shown in Fig. 3.

In summary, we have demonstrated atomic coherence at probe durations as long as 8 s between optical resonances of two  $^{27}\text{Al}^+$  ions held in separate traps. The contrast  $1/e$  decay time of  $t_d = 19 \pm 11$  s is consistent with the 20.6 s excited-state lifetime (corresponding to  $2.3 \times 10^{16}$  optical cycles). Coherence at this level is sufficient to reach a

ratio measurement instability below  $3 \times 10^{-16}/\sqrt{\tau/s}$  for averaging times  $\tau \gg T_R$ . This stability supports a relative frequency measurement with statistical uncertainty  $1 \times 10^{-18}$  in a single day of averaging.

Correlation spectroscopy between spatially separate atomic clocks can improve measurement precision for many applications of optical clocks in which a direct atom-atom comparison is needed. For example, relativistic geodesy measures the gravitational potential difference between two geographical locations by observing a relative frequency shift between atoms located at those points [2]. This has been proposed as an alternative to existing geodetic survey techniques with potential advantages in terms of spatial and temporal resolution. By extending the probe duration beyond the laser coherence limit, future geodetic surveys could use portable laser systems with relatively poor stability compared to the best laboratory systems but still average quickly to the limits imposed by clock accuracy. Similarly, extensions of this technique [31,32] to optical clocks based on different atomic species could be used to measure or constrain the time variation of fundamental constants and to search for ultralight dark matter [3]. These searches can achieve greater resolution by avoiding laser noise limits.

We thank Daniel Cole and Raghavendra Srinivas for their careful reading and feedback on this manuscript. This work was supported by NIST, DARPA, and ONR (Grant No. N00014-18-1-2634). M.E.K. was supported by an appointment to the Intelligence Community Postdoctoral Research Fellowship Program at NIST administered by ORISE through an interagency agreement between the DOE and ODNI. S.M.B. was supported by ARO through Multidisciplinary University Research Initiative Grant No. W911NF-11-1-0400. The views, opinions, and/or findings expressed are those of the authors and should not be interpreted as representing the official views or policies of the Department of Defense or the U.S. Government.

\*ethan.clements@nist.gov

†Present address: Honeywell Quantum Solutions, Broomfield, Colorado 80021, USA.

‡Present address: Colorado State University, Fort Collins, Colorado 80523, USA.

§Present address: IonQ Inc., College Park, Maryland 20740, USA.

||david.hume@nist.gov

- [1] F. Riehle, P. Gill, F. Arias, and L. Robertsson, *Metrologia* **55**, 188 (2018).
- [2] T. E. Mehlstäubler, G. Grosche, C. Lisdat, P. O. Schmidt, and H. Denker, *Rep. Prog. Phys.* **81**, 064401 (2018).
- [3] M. S. Safronova, D. Budker, D. DeMille, D. F. Jackson Kimball, A. Derevianko, and C. W. Clark, *Rev. Mod. Phys.* **90**, 025008 (2018).
- [4] A. D. Ludlow, M. M. Boyd, J. Ye, E. Peik, and P. O. Schmidt, *Rev. Mod. Phys.* **87**, 637 (2015).
- [5] E. Riis and A. G. Sinclair, *J. Phys. B* **37**, 4719 (2004).
- [6] I. D. Leroux, N. Scharmhorst, S. Hannig, J. Kramer, L. Pelzer, M. Stepanova, and P. O. Schmidt, *Metrologia* **54**, 307 (2017).
- [7] W. M. Itano, J. C. Bergquist, J. J. Bollinger, J. M. Gilligan, D. J. Heinzen, F. L. Moore, M. G. Raizen, and D. J. Wineland, *Phys. Rev. A* **47**, 3554 (1993).
- [8] G. J. Dick, J. D. Prestage, C. A. Greenhall, and L. Maleki, in *Proceedings of the 19th Precise Time and Time Interval (PTTI) Applications and Planning Meeting, Redondo, California* (National Aeronautics and Space Administration, Washington, 1987), pp. 133–147.
- [9] D. G. Matei, T. Legero, S. Hafner, C. Grebing, R. Weyrich, W. Zhang, L. Sonderhouse, J. M. Robinson, J. Ye, F. Riehle, and U. Sterr, *Phys. Rev. Lett.* **118**, 263202 (2017).
- [10] M. Takamoto, T. Takano, and H. Katori, *Nat. Photonics* **5**, 288 (2011).
- [11] M. Schioppo, R. C. Brown, W. F. McGrew, N. Hinkley, R. J. Fasano, K. Beloy, T. H. Yoon, G. Milani, D. Nicolodi, J. A. Sherman, N. B. Phillips, C. W. Oates, and A. D. Ludlow, *Nat. Photonics* **11**, 48 (2017).
- [12] E. Oelker, R. B. Hutson, C. J. Kennedy, L. Sonderhouse, T. Bothwell, A. Goban, D. Kedar, C. Sanner, J. M. Robinson, G. E. Marti, D. G. Matei, T. Legero, M. Giunta, R. Holzwarth, F. Riehle, U. Sterr, and J. Ye, *Nat. Photonics* **13**, 714 (2019).
- [13] N. F. Ramsey, *Molecular Beams* (Oxford University Press, London, 1956).
- [14] T. Rosenband, D. Hume, C.-W. Chou, J. Koelemeij, A. Brusch, S. Bickman, W. Oskay, T. M. Fortier, J. Stalnaker, S. A. Diddams *et al.*, in *Frequency Standards and Metrology* (World Scientific, Singapore, 2009), pp. 20–33.
- [15] See Supplemental Material at <http://link.aps.org/supplemental/10.1103/PhysRevLett.125.243602> for an elaboration of details in this paper.
- [16] M. Chwalla, K. Kim, T. Monz, P. Schindler, M. Riebe, C. Roos, and R. Blatt, *Appl. Phys. B* **89**, 483 (2007).
- [17] S. Olmschenk, K. C. Younge, D. L. Moehring, D. N. Matsukevich, P. Maunz, and C. Monroe, *Phys. Rev. A* **76**, 052314 (2007).
- [18] C. W. Chou, D. B. Hume, M. J. Thorpe, D. J. Wineland, and T. Rosenband, *Phys. Rev. Lett.* **106**, 160801 (2011).
- [19] T. R. Tan, R. Kaewuam, K. J. Arnold, S. R. Chanu, Z. Zhang, M. S. Safronova, and M. D. Barrett, *Phys. Rev. Lett.* **123**, 063201 (2019).
- [20] R. Shaniv, N. Akerman, T. Manovitz, Y. Shapira, and R. Ozeri, *Phys. Rev. Lett.* **122**, 223204 (2019).
- [21] T. Manovitz, R. Shaniv, Y. Shapira, R. Ozeri, and N. Akerman, *Phys. Rev. Lett.* **123**, 203001 (2019).
- [22] G. E. Marti, R. B. Hutson, A. Goban, S. L. Campbell, N. Poli, and J. Ye, *Phys. Rev. Lett.* **120**, 103201 (2018).
- [23] A. W. Young, W. J. Eckner, W. R. Milner, D. Kedar, M. A. Norcia, E. Oelker, N. Schine, J. Ye, and A. M. Kaufman, [arXiv:2004.06095](https://arxiv.org/abs/2004.06095).
- [24] T. Rosenband, P. O. Schmidt, D. B. Hume, W. M. Itano, T. M. Fortier, J. E. Stalnaker, K. Kim, S. A. Diddams, J. C. J.

- Koelemeij, J. C. Bergquist, and D. J. Wineland, *Phys. Rev. Lett.* **98**, 220801 (2007).
- [25] P. O. Schmidt, T. Rosenband, C. Langer, W. M. Itano, J. C. Bergquist, and D. J. Wineland, *Science* **309**, 749 (2005).
- [26] S. M. Brewer, J.-S. Chen, A. M. Hankin, E. R. Clements, C. W. Chou, D. J. Wineland, D. B. Hume, and D. R. Leibbrandt, *Phys. Rev. Lett.* **123**, 033201 (2019).
- [27] Y. Colombe, D. H. Slichter, A. C. Wilson, D. Leibfried, and D. J. Wineland, *Opt. Express* **22**, 19783 (2014).
- [28] L.-S. Ma, P. Jungner, J. Ye, and J. L. Hall, *Opt. Lett.* **19**, 1777 (1994).
- [29] J. Ye, J.-L. Peng, R. J. Jones, K. W. Holman, J. L. Hall, D. J. Jones, S. A. Diddams, J. Kitching, S. Bize, J. C. Bergquist, L. W. Hollberg, L. Robertsson, and L.-S. Ma, *J. Opt. Soc. Am. B* **20**, 1459 (2003).
- [30] B. Efron, in *Breakthroughs in Statistics: Methodology and Distribution*, Springer Series in Statistics, edited by S. Kotz and N. L. Johnson (Springer, New York, 1992), pp. 569–593.
- [31] D. B. Hume and D. R. Leibbrandt, *Phys. Rev. A* **93**, 032138 (2016).
- [32] S. Dörscher, A. Al-Masoudi, M. Bober, R. Schwarz, R. Hobson, U. Sterr, and C. Lisdat, [arXiv:1911.13146](https://arxiv.org/abs/1911.13146).